Parallel and Perpendicular Orientation in a Thermotropic Main-Chain Liquid-Crystalline Polymer

Juan P. Fernández-Blázquez, Antonio Bello, and Ernesto Pérez*

Instituto de Ciencia y Tecnología de Polímeros (CSIC), Juan de la Cierva 3, 28006 Madrid, Spain

Received October 6, 2006; Revised Manuscript Received November 16, 2006

ABSTRACT: The orientational behavior of a thermotropic poly(ether ester), PH31B32, with biphenyl units as mesogens and spacers with methyl substituents, has been analyzed. This polymer is one of the few mesophase-forming systems where the amorphous phase can be easily quenched from the isotropic melt. Moreover, under certain conditions the mesophase of this polymer is able to exhibit an anomalous orientation with the molecular axes perpendicular to the uniaxial deformation direction. Specimens of PH31B32 both in the amorphous state or in the smectic mesophase have been studied by stress−strain and fiber X-ray diffraction experiments. In the first case, a fast strain-induced liquid crystallization was observed. In the second case, several strain rates and deformation temperatures have been tested in order to map out the conditions for obtaining the two different kinds of orientation. From the diffraction results, obtained at a final deformation of 300%, those conditions have been approximately defined, leading to a region (at "intermediate" stretching temperatures and strain rates) of mixed orientations. Exclusively parallel orientation is obtained at low deformation temperatures and high strain rates, while the region with 100% perpendicular orientation will appear at rather low strain rates and high temperatures, outside the detection limit of the dynamometer, and overlapping with the isotropization of the mesophase. A model for the two kinds of orientation, based on the hierarchical structure of liquid-crystalline polymers, is proposed.

Introduction

The wide variety of favorable properties (including mechanical properties, dimensional stability, low gas permeability, etc.) and the option to tailor them with simple variations in the structure are two of the most relevant aspects for the industrial and academic interest in liquid-crystalline polymers (LCPs). Moreover, their particular hierarchical structure, with different levels of organization, and its correlation with the final properties are also an attractive aspects of these systems.[1]

One of the most interesting applications of LCPs is the production of high modulus fibers, taking advantage of the inherent anisotropy of the constituent molecular chains. Evidently, as in any kind of fiber, the ultimate properties depend upon the degree of orientation achieved, and considerably high moduli can be obtained along the polymer chains.

But there is a price to pay for enhanced properties in the direction of the chain: the deterioration of those properties in the perpendicular direction.[2,3] Evidently, these statements apply to those cases of "normal" orientation, where the molecular chains are aligned preferentially in the direction parallel to the deformation process.

However, it has been reported that some LCPs with smectic or nematic mesophases may exhibit, under particular circumstances of uniaxial stretching or shear deformation, a kind of anomalous orientation,[4−9] where the chain axes are perpendicular to the stretching direction. As a consequence, the best mechanical properties in such systems are found in the direction normal to the fiber.[5] New prospects are, therefore, envisaged from this particular behavior.

We have recently synthesized[10,11] a new poly(ether ester) with the biphenyl unit as mesogen and two different methyl-substituted trimethylene spacers. This polymer, named as PH31B32, has the structural unit depicted in Figure 1. The thermal, structural, and dynamic-mechanical characterization of this polymer shows that it can be easily prepared in either the pure isotropic amorphous state or in a low ordered smectic mesophase,[10,11] so that the two pure phases can be characterized. For instance, the DSC and DMTA results indicate that the two phases show well different glass transition temperatures.

The aim of the present study is to analyze the orientational behavior of PH31B32. Both amorphous and liquid-crystalline specimens are tested in stress−strain and X-ray diffraction experiments, and different deformation rates and temperatures are investigated in order to map out the conditions for obtaining the two different kinds of orientation, since it is presumed that those conditions will depend very much on the particular characteristics of the different LCPs.

Experimental Section

The details for the synthesis and characterization of PH31B32 have been previously reported.[10] In short, the monomer 1,3-bis(4-diethyloxycarbonyl-4′-biphenyloxy)-1-methylpropane was obtained from ethyl 4′-hydroxy-4-biphenylcarboxylate and (*R*,*S*)-1,3-butanediol, under Mitsunobu conditions.[12] The polymer PH31B32 (see structure in Figure 1) was obtained by melt transesterification of the monomer with 2-methyl-1,3-propanediol using tetraisopropyl titanate as catalyst. The purified polymer was found to have an intrinsic viscosity of 0.681 dL/g (measured at 30 °C in chloroform by using an Ubbelohde viscometer).

Size-exclusion chromatography data were obtained using a Waters 150C gel permeation chromatograph, equipped with two detectors: the conventional refractive index concentration detector and a viscometer Retrofit GPC 150R from Viscotek Co. After a universal calibration (from measurements in different polystyrene standards, using chloroform as eluent at 25 °C), the obtained molecular weight values are $M_w = 43\,600$ and $M_n = 20\,600$.

A film of the polymer was obtained by compression-molding in a Collin press between hot plates (180 °C) at a pressure of 1.5 MPa and subsequently cooling down to room temperature between water-cooled plates in the press. This sample is found to be amorphous. Part of this amorphous film was annealed in an oil bath at 115 °C for 24 h. Under these conditions, a low-ordered smectic mesophase is obtained.[10,11]

* Corresponding author. E-mail: ernestop@ictp.csic.es.

10.1021/ma062312d CCC: $37.00
Published on Web 01/04/2007

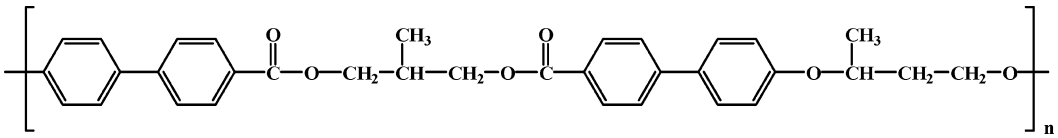

Figure 1. Structural unit of PH31B32.

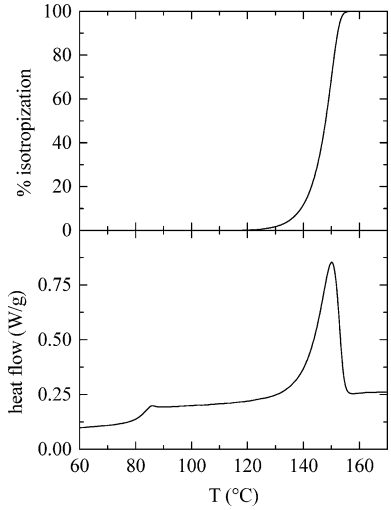

Figure 2. DSC melting curve of a liquid-crystalline specimen of PH31B32 (lower) and relative integral curve corresponding to the isotropization endotherm (upper).

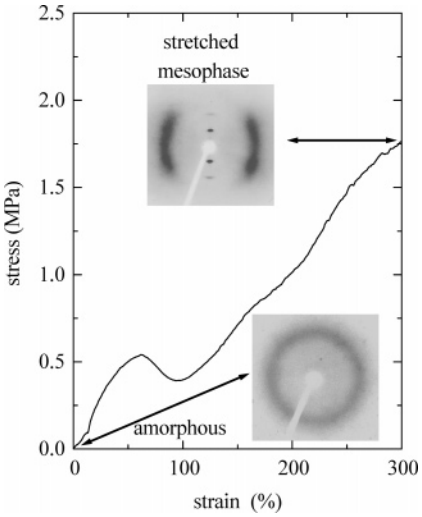

Figure 3. Stress−strain curve corresponding to the uniaxial stretching at 100 °C of an amorphous specimen of PH31B32 with a strain rate of 0.67 min^{-1}. The X-ray fiber diffractograms of the initial stage (amorphous specimen) and of the final stage (stretched mesophase) are inserted (fiber direction: vertical).

Differential scanning calorimetric measurements were carried out with a Perkin-Elmer DSC7 calorimeter connected to a cooling system, at a heating rate of 20 °C/min.

The stress−strain curves were determined using a Minimat 2000 dynamometer. The specimens for these experiments were punched out from the polymer films, either amorphous or in the liquid-crystalline state. The dimensions of these specimens were around 13 mm long, 6 mm wide, and 0.35 mm thick. In a first set of experiments, two specimens, amorphous and liquid crystalline, were uniaxially stretched at 100 °C with a strain rate of 0.67 min^{-1}. In a second set, liquid-crystalline specimens were stretched at different temperatures and strain rates. All the samples were stretched until a final strain of 300%.

Wide-angle X-ray diffraction photographs of the oriented fibers were taken at room temperature using a flat-plate camera attached to a Phillips 2 kW tube X-ray generator using nickel-filtered Cu Kα radiation. The distance from sample to the film (around 7.1 cm) was determined by using aluminum foil as standard. X-ray photographs of selected specimens were obtained with synchrotron radiation in the soft-condensed matter beamline A2 at Hasylab (Hamburg, Germany), by using an image plate detector, located at a distance of 20.5 cm from the sample.

Results and Discussion

Usually, it is rather difficult to quench the isotropic melt to an amorphous glass when liquid-crystal formation is possible, and extraordinary quenching techniques may be needed. However, recent work in our laboratory has been directed to reduce the tendency of the elongated LCP chains to build the supramolecular mesophase structure by decreasing the geometrical and structural symmetry of the constituent molecules. This has been attained in PH31B32, where the mesogens are biphenyl groups, and spacers with an odd number of methylene units and with methyl substituents are used. These methyl groups introduce structural irregularity not only because of the lowering of the intrachain interactions[13] but also due to the random distribution of head-to-head and head-to-tail sequences along the polymer backbone (see Figure 1).

The result is that PH31B32 develops a low-ordered mesophase with a rather slow rate of formation[10,11] in such a way that the isotropic melt of this polymer can be easily quenched into the glassy amorphous state, and considerably high annealing times at temperatures above the glass transition (and below the isotropization temperature) are necessary to develop such a mesophase. As indicated above, an annealing at 115 °C during 24 h was chosen for obtaining the smectic mesophase.

The DSC melting curve corresponding to such annealed sample is shown in the lower part of Figure 2. Two transitions are observed: the glass transition of the smectic glass, centered at 84 °C, and the isotropization of the mesophase, exhibiting a peak temperature of 150 °C and a total enthalpy of 18.2 J/g. The corresponding integral curve of this isotropization endotherm is shown in the upper part of Figure 2, where it can be observed that a very minor, but appreciable, amount of isotropization is already present at temperatures as low as 125−130 °C. On the contrary, the initial quenched film of PH31B32, which is completely amorphous, exhibits only the glass transition in the corresponding DSC scan,[10] now at 95 °C.

The first stress−strain experiment was performed in an amorphous specimen. At room temperature, and at any temperature below T_g, the specimens are too brittle to be analyzed, so that the informative experiments have to be carried out above T_g. Figure 3 shows the stress−strain behavior of an amorphous specimen stretched at 100 °C. After an initial elastic region, characterized by a Young modulus, E, of around 1.6 MPa, a yielding point is observed, with a yield stress, σ_y, of 0.54 MPa (see Table 1), followed by a rather remarkable strain hardening, in such a way that the stress rises to 1.76 MPa for a 300% deformation.

The cause of this hardening is found when analyzing the X-ray diffractograms, which are also shown in Figure 3. The lower photograph corresponds to the initial amorphous sample where only the amorphous isotropic halo, centered at around 0.47 nm, is observed. The photograph at the top of Figure 3

Table 1. Mechanical Parameters (Young Modulus, E, and Yield Stress, σ_y) and Order Parameter for the Uniaxial Stretching at 100 °C of Two Specimens of PH31B32 Which Are, Initially, Amorphous and Liquid Crystalline, Respectively; Only Parallel Orientation Is Observed

	deformation parameters				
sample initial state	T (°C)	strain rate (min^{-1})	E (MPa)	σ_y (MPa)	order parameter (parallel)
amorphous	100	0.67	1.6	0.54	0.96 ± 0.01
mesophase	100	0.67	12.5	2.19	0.93 ± 0.01

corresponds to the stretched fiber, at the end of the experiment. The diagram shows now a narrow spot (and its second order) in the meridian, and the outer diffraction at higher angles is split into two maxima, above and below the equator. This pattern is characteristic of a smectic mesophase with consecutive mesogens arranged in an alternating antiparallel fashion[14−19] (SmC_{alt} mesophase), typical for polybibenzoates with odd spacers. The narrow lower angle diffraction corresponds to the spacing between smectic layers (with a value of 1.26 nm). Since it appears in the meridian, it follows that the molecular axes are aligned parallel to the stretching direction; i.e., a "normal" orientation has been developed.

It is important to mention that, starting from an amorphous specimen, the mesophase has been obtained in the few minutes of the deformation experiment (4.5 min). However, it was shown before[10] that several hours is needed to develop the mesophase just by effect of the temperature. The present process can be termed, therefore, as strain-induced liquid crystallization, in analogy with the well-known strain-induced crystallization reported for semicrystalline polymers.[20−25]

A second experiment was performed on a specimen of PH31B32 which has been annealed at 115 °C for 24 h. Under these annealing conditions, the smectic mesophase has been formed, as it can be observed in the X-ray photograph at the bottom of Figure 4. This photograph shows the two lower angle narrow diffractions, corresponding to the smectic layer spacing (at 1.26 nm) and its second order, and the outer amorphous-like halo.

The stress−strain curve corresponding to this liquid-crystalline specimen is also shown in Figure 4. This curve is quite different than the one for the amorphous sample in Figure 3. First, a considerably higher Young modulus is obtained (12.5 MPa compared with the 1.6 MPa for the amorphous specimen, as seen in Table 1), and also the yield stress is much higher (2.19 MPa instead of the 0.54 MPa in Figure 3), reflecting the significantly higher order of the smectic mesophase. Moreover, the stress after yielding keeps approximately constant, although it is now not very different than the one at the end of the strain hardening of the amorphous sample. This is not surprising since the two ultimate morphologies are rather similar: on stretching, it was shown that the amorphous sample presents strain-induced liquid crystallization, and in fact, the photograph at the top of Figure 4 is practically the same than that obtained from the amorphous specimen after stretching (photograph at the top of Figure 3). Both photographs are characteristic of a SmC_{alt} mesophase, and in both cases a "normal" orientation of the polymer chains in relation to the stretching direction is obtained.

A deeper insight into the analogies and/or differences between the structures obtained by stretching the two different PH31B32 specimens has been obtained from both radial and azimuthal integration of the corresponding X-ray photographs. Obviously, the unoriented samples are of rather little information, so that such integrations have been performed on the stretched fiber photographs.

The radial integrations, in the region of the smectic layer spacing, for the photographs of the two stretched specimens of PH31B32 are shown in Figure 5. It can be observed that although the widths are slightly different, however, the two samples exhibit the same layer spacing: 1.26 nm. The structural unit of PH31B32, shown in Figure 1, is calculated to have an extended chain length of 2.89 nm.[10] However, since it includes two alternating spacers of not very different length,[10] it can be expected that a single-layer smectic structure is exhibited, with a spacing corresponding to about one-half of the total repeat unit, as a result of the random mixing and accommodation of the two spacers.[10,26]

Anyway, both specimens exhibit narrow peaks, so that the different layers retain a rather exact periodicity. However, only the second order is observed, with an intensity around 15% of that for the first-order peak, indicating that the molecules within the layers are imperfectly arranged.[3]

Additional relevant information is obtained from the azimuthal integration of the X-ray diffractograms of the fibers. Figure 6a shows the corresponding integrations in the region of the smectic layer peak. As mentioned before, the two specimens exhibit a maximum of intensity at an angle of 0° in relation to the meridian of the photographs, indicating a "normal" orientation of the molecules: they are arranged parallel to the stretching direction.

Another important parameter that can be determined from the azimuthal integration in Figure 6a is the order parameter. The average degree of orientation of the LC layers with respect to the stretching direction can be represented by the order parameter, which can be related to the spherical harmonics of the probability distribution,[3] similarly to the case of the Hermans orientation function for semicrystalline polymers. It is usual to neglect the higher harmonics, and thus the order parameter, S, is equivalent to the second harmonic, P_2, according to

$$\langle P_2 \rangle = (3\langle \cos^2 \alpha \rangle - 1)/2 \tag{1}$$

where α is the azimuthal angle in relation to the meridian, i.e., the stretching direction. The average on the right-hand of eq 1 can be determined from the intensity distribution, $I(\alpha)$, as follows:[27,28]

$$\langle \cos^2 \alpha \rangle = \frac{\int_0^{\pi/2} I(\alpha) \cos^2 \alpha |\sin \alpha| \, d\alpha}{\int_0^{\pi/2} I(\alpha) |\sin \alpha| \, d\alpha} \tag{2}$$

Therefore, a perfectly uniaxially oriented sample will have $S = 1$, while a completely isotropic sample is characterized by $S = 0$.

By applying eqs 1 and 2 to the data in Figure 6a, the values of 0.96 and 0.93 are obtained for the order parameter of the samples stretched from the amorphous and from the liquid-crystalline specimens, respectively, of PH31B32, as reflected in Table 1. In both cases, therefore, rather perfect orientations of the smectic layers are attained, slightly better in the case of the initially amorphous specimen. The magnitude of the errors reported in Table 1 (and in Table 2) for the order parameter was determined just from the different values obtained from the peaks at azimuthal angles of 0° and 180° (90° and 270° for the perpendicular orientation).

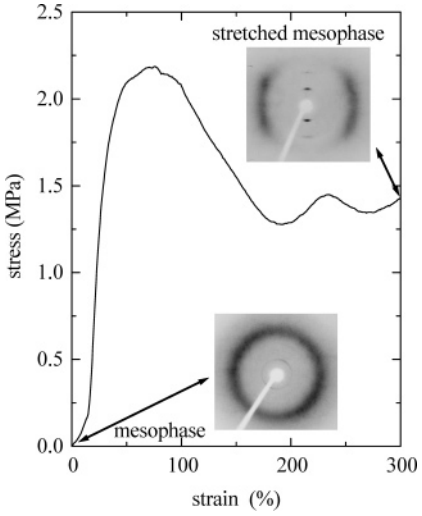

Figure 4. Stress−strain curve corresponding to the uniaxial stretching at 100 °C of a liquid-crystalline specimen of PH31B32 with a strain rate of 0.67 min^{-1}. The X-ray fiber diffractograms of the initial stage (unoriented mesophase) and of the final stage (stretched mesophase) are inserted (fiber direction: vertical).

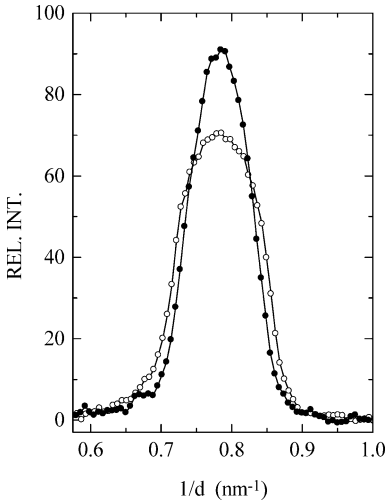

Figure 5. Results for the radial integration, in the region of the layer spacing, of the X-ray photographs for the two stretched specimens of PH31B32 at the top of Figures 3 (open symbols) and 4 (solid symbols).

On the other hand, Figure 6b shows the azimuthal integration in the region of higher angles, i.e., the region of the amorphous-like halo of the mesophase. As commented above, this wide peak appears split below and above the equator. Specifically, the distribution curves in Figure 6b exhibit two maxima at azimuthal angles of around 69° and 111°. This is characteristic of a SmC_{alt} mesophase with consecutive mesogens in an alternating antiparallel arrangement,[14] forming an angle of around +21 or −21° in relation to the molecular axis.

Additional experiments were performed on liquid-crystalline PH31B32 specimens, directed to analyze the conditions necessary to obtain, eventually, a perpendicular anomalous orientation of the polymer chains. Several experiments were carried out at different temperatures and rates of deformation, in samples of PH31B32 that were previously annealed for 24 h at 115 °C; i.e., all of them exhibit from the beginning the SmC_{alt} mesophase. In all cases, the relative amount of each type of orientation was determined from the X-ray diffractograms obtained in the fibers stretched until a 300% deformation.

The results show that appreciable amounts of perpendicular orientation are observed at deformation temperatures above 110

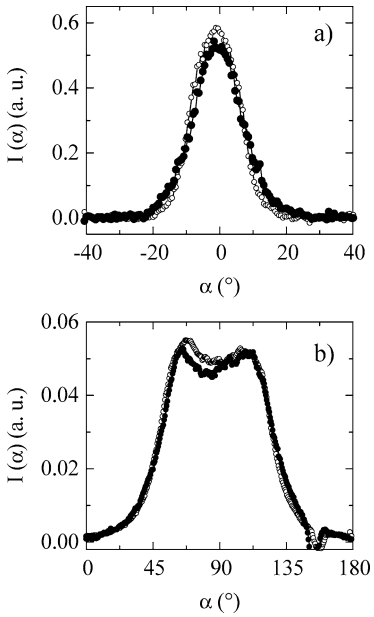

Figure 6. Results for the azimuthal integration, in the region of the layer spacing (a) and of the wide-angle amorphous-like halo (b), of the X-ray photographs for the two stretched specimens of PH31B32 at the top of Figures 3 (open symbols) and 4 (solid symbols). The origin for the azimuthal angle α has been taken in the meridian (stretching direction).

°C, for the tested deformation rates. Particularly interesting are the results obtained when stretching at 120 °C. The stress−strain curves at three well different strain rates are shown in Figure 7. The three curves are rather similar in shape, although the values for the Young modulus and yield stress are rather different, as observed in Table 2.

More revealing are the 2D X-ray photographs acquired at the end of those three tests: as observed in Figure 8, parallel orientation is obtained for the highest deformation rate, while predominantly perpendicular, anomalous, orientation is exhibited for the lower strain rates. The type and degree of orientation can be quantified from the corresponding azimuthal integrations in the region of the smectic layer peak, which are presented in Figure 9a. It can be observed that around 98% of normal, parallel, orientation is obtained for the strain rate of 0.91 min^{-1}, while that percentage decreases to around 19% and 10%, respectively, for the strain rates of 0.091 and 0.0091 min^{-1}. It is evident, therefore, that the anomalous perpendicular orientation is favored by the lower strain rates and the higher deformation temperatures.

The order parameters deduced from the azimuthal intensity distributions in Figure 9a are collected in Table 2, for both the parallel and perpendicular orientations. It can be observed that, in general, the order parameter is higher in the case of parallel normal orientation, although rather high values of the order parameter (around 0.9) are also obtained when the perpendicular orientation is predominant.

Regarding the amorphous-like peak at wide angles, the corresponding azimuthal integrations are shown in Figure 9b. Again, the better "resolution" of the two split peaks reveals a slightly better degree of orientation for the higher strain rate, when parallel orientation is predominantly obtained. It is also interesting to note that now the split spots of the amorphous-like halo are located at around 26° above are below the equator (azimuthal angles of 64° and 116°) for the sample with parallel orientation, instead of the 21° found before. It seems, therefore, that the tilt angle increases as the deformation temperature

Table 2. Mechanical Parameters (Young Modulus, E, and Yield Stress, σ_y) and Order Parameters for the Uniaxial Stretching at 120 °C and Different Strain Rates of Liquid-Crystalline Specimens of PH31B32; Both Parallel and Perpendicular Orientations Are Observed

	deformation parameters				order parameter	
sample initial state	T (°C)	strain rate (min^{-1})	E (MPa)	σ_y (MPa)	parallel	perpendicular
mesophase	120	0.91	6.2	0.45	0.94 ± 0.01	
mesophase	120	0.091	2.7	0.15	0.94 ± 0.03	0.89 ± 0.02
mesophase	120	0.0091	1.2	0.08		0.92 ± 0.02

increases. Moreover, this angle takes the value of 28° and 30° in the specimens with predominantly perpendicular orientation (now at the right or at the left of the meridian), so that the tilting of the mesogens in relation to the molecular axis is higher in this case.

Regarding the experiments when stretching at other temperatures, it has to be pointed out that above 120 °C the isotropization is beginning to occur, as reflected in Figure 2. Moreover, the forces involved are then so low that they cannot be accurately measured by the dynamometer, so that 120 °C is the upper limit.

On the contrary, we have performed several experiments at lower stretching temperatures. Three selected photographs are shown in Figure 10. It can be observed, first, that even at very low strain rates only parallel orientation is obtained when stretching at 105 °C. (For the present sample geometry, the lowest strain rate attained by the dynamometer is around 0.006 min^{-1}, but we decided to stay slightly above that lower limit.) However, a certain amount of perpendicular orientation is produced when stretching at 110 °C and low strain rates, as observed in Figure 10.

All the relevant results for the different tested stretching temperatures and strain rates are collected in Figure 11, where each point represents the actual conditions of the experiment, and the number above them are the percentages of parallel orientation deduced from the corresponding radial integrations. From these values, the conditions for obtaining each type of orientation can be approximately defined, leading to a region (at "intermediate" stretching temperatures and strain rates) of mixed orientations. The "lower" boundary of this mixed region can be defined rather accurately from these results, so that the zone with exclusively parallel orientation is well-defined.

On the contrary, the region with 100% perpendicular orientation is not so accurately defined, since, as commented above, it appears at those conditions of rather low strain rates and high temperatures outside the detection limit of the dynamometer and overlapping with the isotropization of the mesophase. Anyway, Figure 11 represents a fairly good mapping of the conditions for obtaining the two kinds of orientation, under the present deformation protocol described in the Experimental Part.

It is important to note that a very interesting aspect is deduced from Figure 11 when comparing to the behavior of other systems reported in the literature. In the present case, it is rather difficult to obtain exclusively perpendicular orientation (rather easy to get the parallel one), while other reported systems,[4−6] under similar deformation conditions, show the opposite behavior: it is necessary to stretch at very low temperatures (close to the glass transition) and at very high strain rates, to obtain exclusively the parallel orientation, while 100% of anomalous orientation is easily produced at moderately higher temperatures, far away from the isotropization of the corresponding mesophase. More information for other systems and conditions is needed to understand these different behaviors.

The final aspect is the visualization of the mechanism for obtaining either type of orientation. The hierarchical structure of low-ordered smectic mesophases of LCPs is reported to consist of different levels[1,29−31] starting from the basic molecular arrangement with the mesogens organized into smectic layers. The order in the arrangement of these smectic layers will be disturbed by the accumulation of paracrystalline distortions, by the random shift inside the layers, or by the regions where segregated defects are concentrated.[1,30,31] Anyway, layered packs with correlation lengths of 10−70 nm are presumed before those interruptions. These dimensions are on the order of the extended chain length: considering the molecular weight and the length of the repeating unit (see above), an extended chain length of around 100 nm is obtained for the present PH31B32 polymer sample. Therefore, and as was shown before from the synchrotron results of this polymer[10] and of another polybibenzoate,[32,33] it seems that the chain folding, if any, is not very extensive in the smectic mesophase.

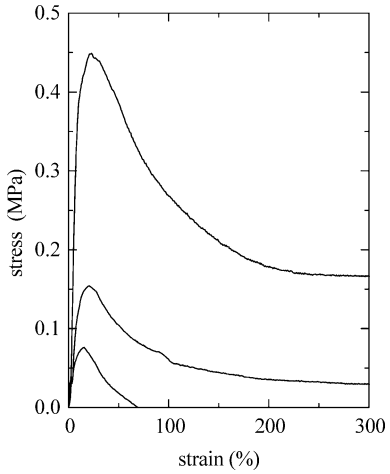

Figure 7. Stress−strain curves corresponding to the uniaxial stretching of liquid-crystalline specimens of PH31B32 at 120 °C and with different strain rates: 0.91 min^{-1} (upper curve), 0.091 min^{-1} (middle curve), and 0.0091 min^{-1} (lower curve).

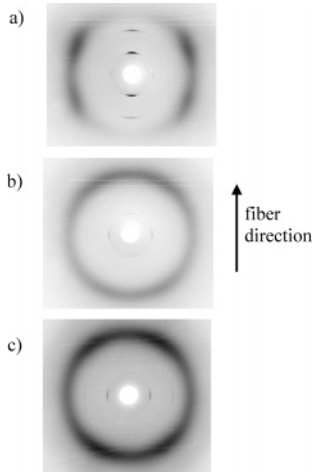

Figure 8. X-ray diffractograms of the fibers after uniaxial stretching (Figure 7) of liquid-crystalline specimens of PH31B32 at 120 °C and with different strain rates: 0.91 (a), 0.091 (b), and 0.0091 min^{-1} (c). Fiber direction: vertical.

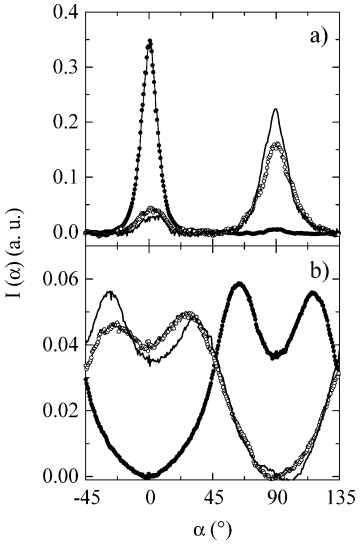

Figure 9. Results for the azimuthal integration, in the region of the layer spacing (a), and of the wide-angle amorphous-like halo (b), of the X-ray photographs for the three specimens of PH31B32 in Figure 8 stretched at different strain rates: 0.91 min^{-1} (solid symbols), 0.091 min^{-1} (open symbols), and 0.0091 min^{-1} (continuous line). The origin for the azimuthal angle α has been taken in the meridian (stretching direction).

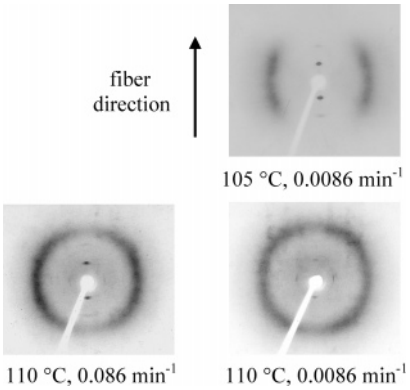

Figure 10. Selected fiber X-ray diffractograms after stretching liquid-crystalline specimens of PH31B32 at the indicated temperatures and strain rates. Fiber direction: vertical.

The next hierarchical level is the assembly of those packs to define domains in the micron size scale. In this structure, each domain will have a characteristic order parameter, which varies slightly with position but may change very much (disclinations) from one domain to the other, the global order parameter being the average of those of all domains.[3] Therefore, the order parameter may be considerably high in a very local scale (inside the domains), in contrast to the much lower value on a global scale.

We can, therefore, envisage the initial structure of our smectic polymer as composed of domains randomly oriented but with a rather "regular" order parameter inside the domains, as depicted in the upper part of Figure 12. (The domains have been pictured as well separated and rather regular, for better visualization, and with a perfect order inside.) If it is assumed that the dimensions of the domains in the lateral directions are considerably larger than in the direction of the molecular axis, it seems reasonable to expect that in the case of low strain rates and/or high deformation temperatures, these domains will be able to slide through the disclinations and reorient in relation to the direction of deformation, following the left pathway of Figure 12 and ending with the largest dimension oriented with

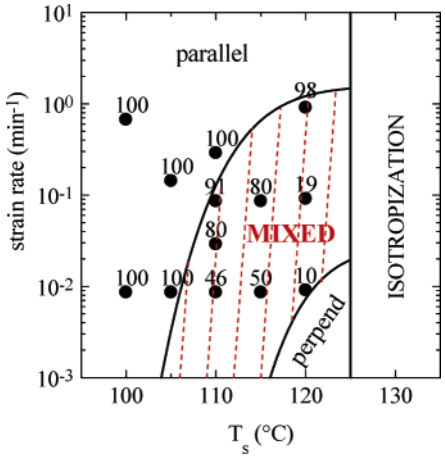

Figure 11. Mapping of the conditions to obtain the two different types of orientation in liquid-crystalline specimens of PH31B32, as a function of stretching temperature and strain rate (for a final deformation of 300%). The points represent the conditions of the different experiments, with the percentage of parallel orientation above them.

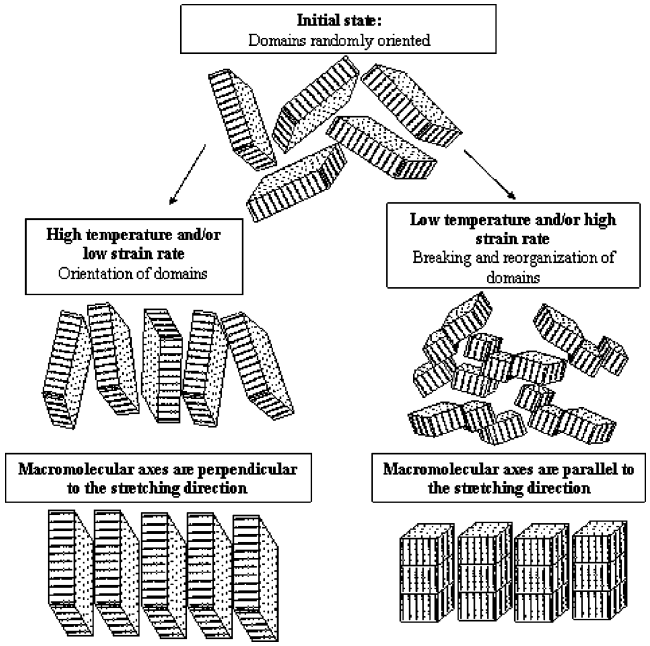

Figure 12. Schematic model for obtaining perpendicular (left pathway) or parallel (right pathway) orientation starting from idealized liquid-crystalline domains. For better visualization, the domains have been pictured as well separated and rather regular.

the deformation, so that the molecular axes are perpendicular to the stretching direction: *anomalous orientation*.

On the contrary, in the case of high strain rates and/or low temperatures, the domains will not be able to follow the deformation, and presumably, they will broke apart and reorganize into some kind of fibrillar structure, ending with the molecular axes parallel to the direction of deformation: *normal orientation*, as in the right pathway of Figure 12.

Irrespectively of the deformation mechanism, it has been shown that it is relatively easy to design the deformation conditions in this PH31B32 liquid-crystalline polymer in order to obtain either type of deformation or a mixture of them. If we consider that the best mechanical properties are always in the molecular axis direction,[5] it means that fibers can be prepared with a tailored balance of properties in the directions parallel and perpendicular to the fiber axis, although, evidently, the

ultimate properties of PH31B32 are far to be considered as a high-performance polymer.

Conclusions

The thermotropic poly(ether ester), PH31B32, with biphenyl units as mesogens and spacers with methyl substituents, is one of the few mesophase-forming systems where the amorphous phase can be easily quenched from the isotropic melt. Moreover, under certain conditions the mesophase of this polymer is able to exhibit an anomalous orientation with the molecular axes perpendicular to the uniaxial deformation direction.

The stress−strain and fiber X-ray diffraction experiments performed on specimens of PH31B32 both in the amorphous state or in the smectic mesophase show that, in the first case, a fast strain-induced liquid crystallization is observed. In the second case, several strain rates and deformation temperatures have been tested in order to map out the conditions for obtaining the two different kinds of orientation. From the diffraction results, obtained at a final deformation of 300%, those conditions have been approximately defined, leading to a region (at "intermediate" stretching temperatures and strain rates) of mixed orientations.

Exclusively parallel (normal) orientation is obtained at low deformation temperatures and high strain rates, while the region with 100% perpendicular orientation will appear at rather low strain rates and high temperatures, outside the detection limit of the dynamometer, and overlapping with the isotropization of the mesophase.

A model for the two kinds of orientation, based on the hierarchical structure of liquid-crystalline polymers, is proposed.

Acknowledgment. The financial support of MEC (Project MAT2004-06999-C02-01) is gratefully acknowledged. J.P.F.-B. is indebted to CSIC for a research grant financed by the I3P program through the Fondo Social Europeo. The synchrotron work was supported by the European Community-Research Infrastructure Action under the FP6 "Structuring the European Research Area" Programme through the Integrated Infrastructure Initiative "Integrating Activity on Synchrotron and Free Electron Laser Science", Contract RII3-CT-2004-506008. We thank the collaboration of the Hasylab personnel, and especially Dr. S. Funari, responsible for the polymer beamline.

References and Notes

(1) MacDonald, W. A. In *Liquid Crystal Polymers: From Structures to Applications*; Elsevier: New York, 1992; Chapter 8, p 407.
(2) Nielsen, L. E.; Landel, R. F. *Mechanical Properties of Polymers and Composites*; Marcel Dekker: New York, 1994.
(3) Donald, A. M.; Windle, A. H. In *Liquid Crystalline Polymers*; Cahn, R. W., Davis, E. A., Ward, I. M., Eds.; Cambridge University Press: Cambridge, 1992.
(4) (a) Bello, P.; Bello, A.; Lorenzo, V. *Polymer* **2001**, *42*, 4449. (b) Bello, P.; Bello, A.; Riande, E.; Heaton, N. *Macromolecules* **2001**, *34*, 181.
(5) Martínez-Gómez, A.; Pereña, J. M.; Lorenzo, V.; Bello, A.; Pérez, E. *Macromolecules* **2003**, *36*, 5798.
(6) (a) Tokita, M.; Osada, K.; Kawauchi, S.; Watanabe, J. *Polym. J.* **1998**, *30*, 687. (b) Tokita, M.; Tokunaga, K.; Funaoka, S.; Osada, K.; Watanabe, J. *Macromolecules* **2004**, *37*, 2527. (c) Osada, K.; Koike, M.; Tagawa, H.; Hunaoka, S.; Tokita, M.; Watanabe, J. *Macromolecules* **2005**, *38*, 7337.
(7) Leland, M.; Wu, Z.; Chhajer, M.; Ho, R.-M.; Cheng, S. Z. D.; Keller, A.; Kricheldorf, H. R. *Macromolecules* **1997**, *30*, 5249.
(8) (a) Ugaz, V. M.; Burghardt, W. R. *Polym. Mater. Sci. Eng.* **1998**, *79*, 369. (b) Zhou, W.-J.; Kornfield, J. A.; Ugaz, V. M.; Burghardt, W. R.; Link, D. R.; Clark, N. A. *Macromolecules* **1999**, *32*, 5581.
(9) (a) Romo-Uribe, A.; Windle, A. H. *Macromolecules* **1993**, *26*, 7100. (b) Romo-Uribe, A.; Windle, A. H. *Macromolecules* **1996**, *29*, 6246.
(10) Fernández-Blázquez, J. P.; Bello, A.; Pérez, E. *Macromolecules* **2004**, *37*, 9018.
(11) Fernández-Blázquez, J. P.; Bello, A.; Pérez, E. *Polymer* **2005**, *46*, 10004.
(12) Mitsunobu, O. *Synthesis* **1981**, 1.
(13) del Campo, A.; Pérez, E.; Benavente, R.; Bello, A.; Pereña, J. M. *Polymer* **1998**, *39*, 3847.
(14) Watanabe, J.; Hayashi, M.; Nakata, Y.; Niori, T.; Tokita, M. *Prog. Polym. Sci.* **1997**, *22*, 1053.
(15) (a) Pérez, E.; Pereña, J. M.; Benavente, R.; Bello, A. Characterization and Properties of Thermotropic Polybibenzoates. In *Handbook of Engineering Polymeric Materials*; Cheremisinoff, N. P., Ed.; Marcel Dekker: New York, 1997; Chapter 25, p 383. (b) Pérez, E. Liquid crystalline polymers: Polyesters of bibenzoic acid. In *The Polymeric Materials Encyclopedia*; Salamone, J. C., Ed.; CRC Press: Boca Raton, FL, 1996; Vol. 5, p 3711.
(16) Abe, A. *Macromolecules* **1984**, *17*, 2280.
(17) Pérez, E.; Riande, E.; Bello, A.; Benavente, R.; Pereña, J. M. *Macromolecules* **1992**, *25*, 605.
(18) Bello, A.; Riande, E.; Pérez, E.; Marugán, M. M.; Pereña, J. M. *Macromolecules* **1993**, *26*, 1072.
(19) Pérez, E.; Benavente, R.; Cerrada, M. L.; Bello, A.; Pereña, J. M. *Macromol. Chem. Phys.* **2003**, *204*, 2155.
(20) Peterlin, A. *Polym. Eng. Sci.* **1976**, *16*, 126.
(21) Yeh, G. S. Y. *Polym. Eng. Sci.* **1976**, *16*, 138. Yeh, G. S. Y. *Polym. Eng. Sci.* **1976**, *16*, 145.
(22) Stein, R. S. *Polym. Eng. Sci.* **1976**, *16*, 152.
(23) LeBourvellec, G.; Monnerie, L.; Jarry, J. P. *Polymer* **1986**, *27*, 856.
(24) Salem, D. R. *Polymer* **1992**, *33*, 3182.
(25) Shepherd, J. E.; McDowell, D. L.; Jacob, K. I. *J. Mech. Phys. Solids* **2006**, *54*, 467.
(26) Watanabe, J.; Nakata, Y.; Simizu, K. *J. Phys. II* **1994**, *4*, 581.
(27) Windle, A. H. In *Developments in Oriented Polymers-1*; Ward, I. M., Ed.; Applied Science Publishers: London, 1982; Chapter 1, p 1.
(28) Baltá-Calleja, F. J.; Vonk, C. G. *X-Ray Scattering of Synthetic Polymers*; Elsevier: Amsterdam, 1989.
(29) Sawyer, L. C.; Jaffe, M. *J. Mater. Sci.* **1986**, *21*, 1897.
(30) Tsukruk, V. V.; Shilov, V. V.; Lipatov, Y. S. *Acta Polym.* **1985**, *36*, 403.
(31) Hu, Y. S.; Schiraldi, D. A.; Hiltner, A.; Baer, E. *Macromolecules* **2003**, *36*, 3606.
(32) Pérez, E.; Todorova, G.; Krasteva, M.; Pereña, J. M.; Bello, A.; Marugán, M. M.; Shlouf, M. *Macromol. Chem. Phys.* **2003**, *204*, 1791.
(33) Todorova, G. K.; Krasteva, M. N.; Pérez, E.; Pereña, J. M.; Bello, A. *Macromolecules* **2004**, *37*, 118.

MA062312D